

**Original Article****Real-Time Intrafraction CBCT Imaging: Commissioning and Clinical Applications in Radiation Therapy**

Deeksha Jaiswal, Monika Goyal, C.P Bhatt

**Abstract:**

**Introduction:** Conventional CBCT is limited to pretreatment imaging, leaving intrafractional motion a challenge. Real-time intrafraction CBCT enables continuous monitoring of tumor motion during radiation delivery, overcoming the limitations of conventional pretreatment CBCT. This study focuses on the commissioning of real-time intrafraction CBCT imaging and evaluating its feasibility with the goal of improving treatment precision, reducing uncertainties, and enhancing patient outcomes.

**Materials and Methods:** In this study, we used the **Catphan 504 phantom (module number TBD)** to evaluate the image quality of intrafraction cone-beam computed tomography (CBCT) imaging during stereotactic body radiotherapy (SBRT) treatment deliveries. Various structures were drawn on the CBCT scans of the CatPhan 504 phantom with the field sizes ranged from **0.5 x 0.5 cm<sup>2</sup> to 9 x 9 cm<sup>2</sup>**, increasing in **5 mm increments**. Each plan is optimized for 5 Gy in single fraction for 6MV photon. It is calculated for grid spacing of 0.2 cm and for statistical uncertainty of 1%. A 5mm small structure plan was created using 858.0 MU. The 90 mm Large structure plan was made with 600.64 MU.

**Results:** The analysis reveals a significant relationship between field size and imaging parameters in real-time intrafraction CBCT imaging. As the field size increases Geometric distortion, CNR, and overall uniformity decline, potentially compromising image accuracy and affecting tumor localization. For both small and large structures, geometric distortion remained minimal (<1 mm) at lower field sizes (5–55 mm) but progressively worsened as field size increased. Spatial resolution improves, enhancing fine detail detection, but maximum HU deviation rises, which may introduce inaccuracies in tissue density representation and setup verification.

**Conclusion:** This study successfully commissioned real-time intrafraction CBCT imaging for various field sizes using the Catphan 504 phantom. The findings demonstrate that real-time CBCT integration enhances the accuracy of dose delivery by effectively accounting for intrafraction motion. This improved precision in radiation therapy can lead to better treatment outcomes and increased patient safety.

**JK-Practitioner2025; 30 (2-3):30-40****INTRODUCTION**

Radiation therapy remains a cornerstone in the treatment of cancer, with its efficacy significantly enhanced through the integration of advanced imaging technologies. Imaging plays a critical role in radiation oncology, aiding in disease identification, understanding tumor biology, staging, and guiding treatment planning and delivery [1, 2]. A variety of imaging modalities, such as computed tomography (CT), magnetic resonance imaging (MRI), ultrasound, and positron emission tomography (PET)-CT, provide detailed insights that are essential for both diagnostic evaluation and precision in radiation therapy treatment planning [3,4].

In recent decades, radiation therapy techniques have evolved, moving from conventional radiotherapy to more advanced methods like intensity-modulated radiotherapy (IMRT), image guided radiotherapy

**Author Affiliations**

Deeksha Jaiswal, Department of Physics, GLA University, Mathura, India. Department of Radiation Oncology, V.M.M.C and Safdarjung Hospital, New Delhi, India. Monika Goyal, Department of Physics, GLA University, Mathura, India., C.P Bhatt, Department of Physics, Sarvodaya Hospital, Faridabad, India.

**Correspondence**

**Deeksha Jaiswal**, Department of Physics, GLA University, Mathura, India. Department of Radiation Oncology, V.M.M.C and Safdarjung Hospital, New Delhi, India. Email: [jaiswaldeeksha102@gmail.com](mailto:jaiswaldeeksha102@gmail.com)

**Indexed**

EMBASE, SCOPUS, IndMED, ESBCO, Google Scholar besides other national and International Databases

**Cite This Article as**

Jaiswal D, Goyal M, Bhat CP, Real-Time Intrafraction CBCT Imaging: Commissioning and Clinical Applications in Radiation Therapy JK Pract 2025; 30 (2-3):30-40

Full length article available at **jkpractitioner.com** one month after publication

**Keywords:** Catphan 504; Radiation therapy; Dose Calculation; Overall uniformity; Tissue Density Representation.

(IGRT), stereotactic body radiotherapy (SBRT), and proton beam therapy (PBT). Image guided radiation therapy (IGRT) is an advanced radiation therapy technique that enhance precision by using real time imaging to accurately target tumors while minimizing damage to healthy tissues. IMRT shapes radiation dose intensity across the tumour. SBRT delivers high dose precise radiation in fewer sessions. These innovations have allowed for higher precision and accuracy in delivering radiation doses to the tumor while minimizing damage to surrounding healthy tissues, leading to better clinical outcomes [5,6]. These techniques rely heavily on accurate imaging for planning and real-time adjustments during treatment to maintain tight margins and deliver higher doses directly to the tumor [7,8].

A major challenge in the delivery of high-precision radiotherapy lies in managing geometric uncertainties, particularly those arising from inter-fraction and intra-fraction motion. Tumor displacement due to respiration, cardiac activity, swallowing, and other physiological movements can lead to deviations in dose delivery, especially in extracranial sites where organ motion is pronounced [9]. Real-time monitoring of tumor position during treatment is thus essential for maintaining dose conformity and ensuring treatment accuracy.

Intra-fraction motion has a direct influence on planning target volume (PTV) margins and dose distribution [10-13]. To mitigate its effects, several techniques for real-time target tracking have been developed. These include sonographic tracking [14], implanted fiducial markers [15,16], beacon transponders [17], and emerging systems such as linear accelerator (LINAC)-integrated MRI [18,19]. Among these, intrafractional ultrasound (US) guidance offers a promising solution by enabling non-invasive, markerless, real-time volumetric tracking during beam delivery. However, ultrasound systems may interfere with dose distribution due to physical presence within the treatment field [20], and have limitations related to imaging through air or bone, and restricted imaging volume rates in some 3D systems [21].

Alternative approaches such as cone-beam computed tomography (CBCT) have also been employed for intrafraction monitoring. Real-time intrafraction CBCT, particularly in the context of magnetic resonance image-guided radiotherapy (MRIGRT), allows continuous visualization of patient anatomy during treatment. However, limitations such as image artifacts, increased acquisition times, and patient motion reduce its effectiveness [22]. Although MRIGRT offers superior soft-tissue contrast and facilitates online adaptation, CBCT-guided adaptation remains more commonly implemented in clinical settings due to workflow compatibility.

Historically, intra-fraction motion has been assessed retrospectively through imaging acquired before or after treatment. While useful, such methods fail to

capture dynamic changes during beam-on time. Real-time intrafraction CBCT addresses this gap by enabling direct imaging during irradiation, thereby supporting adaptive interventions that enhance treatment precision and reduce uncertainties.

This study focuses on the commissioning of real-time intrafraction CBCT imaging and evaluating its feasibility for clinical treatments in radiation oncology. By incorporating real-time CBCT into clinical workflows, radiation oncologists can gain more precise control over intra-fraction movements, ultimately leading to more accurate dose delivery and improved patient outcomes. The feasibility of integrating this technology into routine clinical practice will be explored, along with its potential impact on reducing uncertainties and enhancing the precision of modern radiation therapy techniques.

The main goal of this study was to evaluate the effect of MV-scattered photons on the image quality of kV intrafraction CBCT. Specifically, we aimed to determine how the presence of MV treatment beams impacted the clarity, resolution, and overall quality of CBCT images used for real-time monitoring during treatment.

By examining these effects, this study seeks to determine the clinical utility of real-time CBCT for monitoring intra-treatment motion and enabling real-time adaptive corrections. The findings will support the optimization of CBCT protocols for stereotactic treatments such as stereotactic radiosurgery (SRS) and stereotactic radiotherapy (SRT), ultimately contributing to improved treatment precision and patient outcomes.

## MATERIALS AND METHODS

### Phantom and analysis software used

In this study, we used the **CatPhan 504 phantom (module number TBD)** to evaluate the image quality of intrafraction cone-beam computed tomography (CBCT) imaging during stereotactic body radiotherapy (SBRT) treatment deliveries [23]. The CatPhan 504 is a widely recognized phantom designed for quality assurance in both diagnostic and radiation therapy imaging. It contains several modules to assess key imaging parameters such as spatial resolution, contrast sensitivity, uniformity, and geometric accuracy, making it an ideal tool for this investigation [24].

We have generated the CBCT protocol for intrafraction CBCT and on the basis of template we have taken the images of the phantom.

Figure 1(a) and (b) is cross-sectional image from Cone Beam Computed tomography (CBCT) scan. The numbers and scale on the image indicate measurement values in millimeters and a grayscale on the right range from -1000 to 1000, which is typical for Hounsfield units used in CT scans, where -1000 represents air and 1000 represent dense bone. The red squares and numbers likely indicate measurement points or regions of interest for analysis. The red

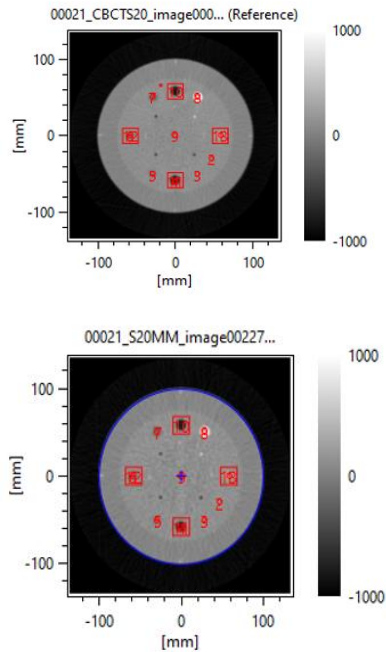


**Fig1(a) Fig1(b)**

Figure 1(a)&(b) represent transverse view of catphan image 1(a) pre cbct image of catphan (reference image), 1(b) Intrafraction cbct image of catphan squares symbol seen in the image, when used in the context of image analysis within computer programming, is commonly referred to as a bounding box or region of interest (ROI). It serves to highlight specific areas within an image that are of particular interest for analysis or processing. Figure 1(a) represent PRECBCT image of CATPHAN which is taken as reference image without MV Beam ON. Fig 1(b) represent intrafraction CBCT image of CATPHAN for 20 mm field size. We have analyzed all the plans using my QA software (IBA Dosimetry, Keyversion: 23.3.1.96402, Germany)

#### **Phantom Structure Design**

In order to thoroughly evaluate the precision and resolution of intrafraction CBCT during treatment, various structures were drawn on the CBCT scans of the CatPhan 504 phantom. The structures are drawn on the image of phantom starting from 5mm small, 5mm large, 10 mm small, 10 mm large in the increment of 5 mm and goes upto 90 mm. For 5 mm small structure radius is kept 5mm and length of the structure is also same 5mm. For 5 mm large structure radius is 5 mm but length of the structure is 10 mm likewise we drawn all the structure. These structures were designed to mimic small tumors or critical anatomical landmarks that require precise targeting in clinical treatments. This variation allowed for a comprehensive assessment of how well intrafraction CBCT could detect and monitor targets of different sizes throughout the treatment process.

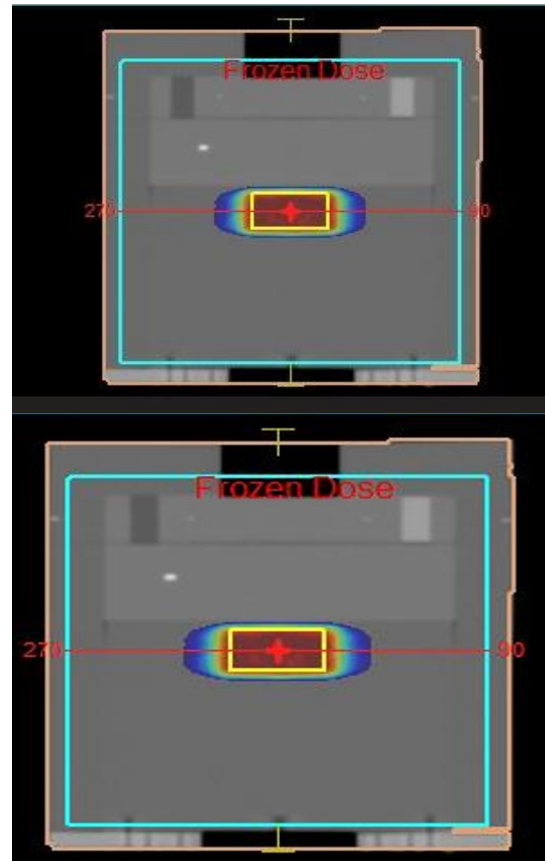


**Figure 2(a) 2mm small structure**  
**Figure2(b) 2mm large structure**

Figure 2(a)&(b) illustrate sagittal view of catphan image 2(a) delineation of 2mm small structure and 2(b) 2 mm large structure

#### **Phantom Alignment and Imaging Setup**

The **CatPhan 504 phantom** was precisely aligned with the isocenter of the Elekta linear accelerator to ensure accurate imaging and radiation delivery. Isocenter alignment is critical in radiotherapy, particularly in SBRT, where sub-millimeter precision is required to avoid damage to surrounding healthy tissue.

The phantom was aligned to the machine's isocenter using established protocols, ensuring that the planned beams and CBCT images were correctly focused on the target structures within the phantom.

#### **Imaging System and parameter**

The **Elekta Versa HD** linear accelerator, equipped with a kilovoltage (kV) CBCT system, was used to acquire both baseline and intrafraction CBCT images. The primary objective was to assess how the image quality of CBCT is impacted during the delivery of radiation with the MV beam on.

- **X-ray tube voltage:** 100 kV
- **X-ray tube current:** 20 mA
- **Gantry rotation:** 360 degrees full arc
- **Field of view (FOV):** S20 small field of view, which provides high-resolution imaging of a localized region for precise monitoring during treatment.

**Table 1** represent plan parameter used in treatment planning with Monitor Unit(MU)

Serial No	Field Size (mm)	Length Y1	Length Y2	MU
1	5 mm LARGE	1.0	1.0	893.15
2	5 mm SMALL	1.0	1.0	858.0
3	10 mm LARGE	1.58	1.57	852.14
4	10 mm SMALL	1.0	1.0	897.81
5	15 mm LARGE	2.0	2.0	823.72
6	15 mm SMALL	1.5	1.5	784.68
7	20 mm LARGE	2.7	2.7	758.85
8	20 mm SMALL	1.5	1.5	819.77
9	25 mm LARGE	3.2	3.20	739.38
10	25 mm SMALL	2.0	2.0	739.30
11	30 MM LARGE	3.7	3.7	728.85
12	30 MM SMALL	2.2	2.2	741.20
13	35 MM LARGE	3.7	3.7	728.85
14	35 MM SMALL	2.5	2.5	737.43
15	40 MM LARGE	4.5	4.5	719.78
16	40 MM SMALL	2.7	2.7	711.98
17	45 MM LARGE	5.5	5.5	678.07
18	45 MM SMALL	3.0	3.0	725.21
19	50 MM LARGE	6.0	6.0	674.04
20	50 MM SMALL	3.2	3.2	716.65
21	55 MM LARGE	6.5	6.5	668.90
22	55 MM SMALL	3.5	3.5	699.70
23	60 MM LARGE	7.0	7.0	660.02
24	60 MM SMALL	4.0	4.0	682.28
25	65 MM LARGE	7.5	7.5	651.78
26	65 MM SMALL	4.0	4.0	680.60
27	70 MM LARGE	8.2	8.2	638.80
28	70 MM SMALL	4.5	4.5	663.94
29	75 mm LARGE	8.7	8.7	623.47
30	75 mm SMALL	4.7	4.7	654.02
31	80 mm LARGE	9.5	9.5	618.64
32	80 mm SMALL	5.0	5.0	641.95
33	90 mm LARGE	10.5	10.5	600.64
34	90 mm SMALL	5.5	5.5	625.74

- A specified maximum of 320 frames were collected for analysis during each full rotation of the gantry, ensuring comprehensive imaging data for evaluation.

#### **Treatment Plans**

For the purpose of this study, we created several full-arc treatment plans on the Elekta Versa HD linear accelerator, which is equipped with CBCT for image guidance. We have created 34 plans for small and large structure on CatPhan CT with different MU and Field size as shown in Table 1.

A full arc plan was made from gantry angle 180 to 180 (CCW) with monaco planning system (Infinity; Elekta Medical Systems, Crawly, UK) (version

6.1.2.0). Dynamic conformal arc plan is created started from gantry angle 180 degree with 360-degree arc, collimator 0-degree, couch 0 degree. Each plan is optimized for 5 Gy in single fraction for 6MV photon. It is calculated for grid spacing of 0.2 cm and for statistical uncertainty of 1%. A 5mm small structure plan was created using 858.0 MU. The 90 mm large structure plan was made with 600.64 MU.

The treatment plans were designed with a dose rate of 600 monitor units (MU) per minute to simulate the conditions typical of SBRT, a treatment method known for delivering highly conformal, high-dose radiation in fewer sessions. To analyze the impact of intrafraction CBCT on different field sizes, the

Monaco treatment planning system was used to generate plans with varying field sizes. The field sizes ranged from 0.5 x 0.5 cm<sup>2</sup> to 9 x 9 cm<sup>2</sup>, increasing in 5 mm increments. This range was chosen to investigate how different field sizes affect image quality and the detection of small structures within the treatment area during CBCT imaging.

#### **Intrafraction-CBCT Acquisition**

For each of the treatment plans, intrafraction CBCT images were acquired using a start and stop gantry angle of 180 degrees, full arc imaging conditions during actual SRS/SRT treatments. These images were collected both with the MV beam off (baseline images) and with the MV beam on (during treatment), allowing for a direct comparison of image quality under treatment conditions. The data from these intrafraction CBCT scans were compared with the baseline scans to determine the extent to which the scatter from MV beam affected the image quality [25].

#### **RESULTS**

The purpose of this study was to evaluate the

**Table 2.1: Intrafraction Large field size 5 mm to 45 mm**

<b>Intrafraction Field Size LARGE(mm)</b>										
<b>PARAMETER</b>	<b>REF VALUE</b>	<b>5 mm</b>	<b>10 mm</b>	<b>15 mm</b>	<b>20 mm</b>	<b>25 mm</b>	<b>30 mm</b>	<b>35 mm</b>	<b>40 mm</b>	<b>45 mm</b>
<b>GEOMETRIC DISTORTION (mm)</b>	-0.42	-0.66	-0.7	-0.81	-1	-1.1	1.12	-1.15	-1.21	-1.22
<b>SPATIAL RESOLUTION (lp/mm)</b>	0.27	0.29	0.3	0.3	0.35	0.35	0.36	0.39	0.37	0.48
<b>OVERALL UNIFORMITY (%)</b>	95.76	96.82	96.51	95.58	94.79	93.86	92.62	93.78	91.57	88.86
<b>MINIMUM UNIFORMITY (%)</b>	95.66	96.75	96.43	95.45	94.59	93.58	92.22	93.49	90.98	87.82
<b>CONTRAST (%)</b>	2.92	7.38	6.55	6	5.61	9.61	6.21	10.02	4.93	12.31
<b>CNR</b>	1.95	0.77	0.87	0.95	1.02	0.59	0.92	0.57	1.16	0.46
<b>MAXIMUM HU DEVIATION (HU)</b>	257.43	258.73	248.71	262.02	273.41	290.71	286.41	290.12	313.51	344.47

In the Table 2.1 large structures of 5 mm were drawn with radius 5 mm and length 10 mm . The field size varies from 0.5x0.5 cm<sup>2</sup> to 9x9 cm<sup>2</sup>. We analyze different imaging parameters for different field size and compare this with image without MV beam ON. In Table 3.1small structures were drawn on cat phan with 5mm radius and 5mm length. The field size varied with increment of 5 mm. We analyze different imaging parameter for different field size. In the table 2.1 it was observed that geometric distortion which is important in CBCT because it affect the quality of resulting image. It can cause size changes, shape distortion, blurring and displacement. Here the geometric distortion explains with the help of the graph which is given below.

increases. Geometric distortion was strongly dependent on field size. For both small and large structures, distortion remained minimal (<-1 mm) at lower field sizes (5–55 mm) but progressively worsened as field size increased. This pattern highlights that larger fields are more vulnerable to scatter contamination, consistent with prior studies reporting that MV scatter alters CBCT geometry during beam-on imaging.

Spatial Resolution (SR) is the ability to distinguish between objects or structures that differ in density. Spatial resolution showed a contrasting trend. In both small and large fields, resolution improved modestly with

**Table2.2: Intrafraction Large field size 50 mm to 90 mm**

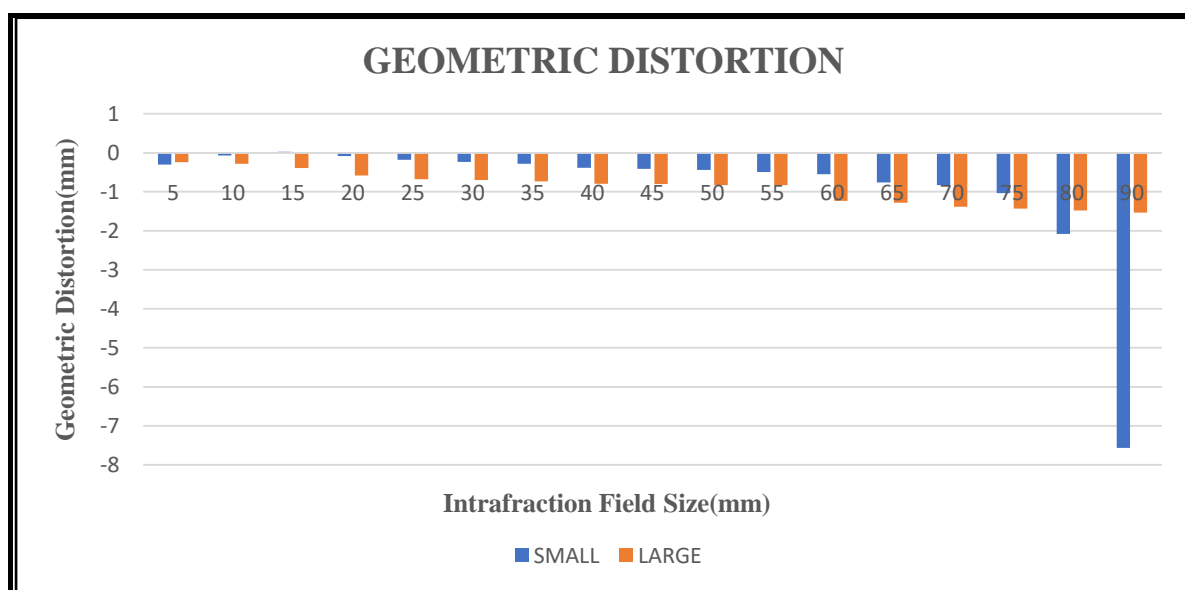
Intrafraction Field Size LARGE (mm)									
PARAMETER	REF VALUE	50 mm	55 mm	60 mm	65 mm	70 mm	75 mm	80 mm	90 mm
GEOMETRIC DISTORTION (mm)	-0.42	-1.25	-1.25	-1.65	-1.7	-1.8	-1.85	-1.9	-1.95
SPATIAL RESOLUTION (lp/mm)	0.27	0.46	0.43	0.31	0.35	0.38	0.37	0.45	0.4
OVERALL UNIFORMITY (%)	95.76	86.79	87.02	85.71	85.41	84.8	83.33	81.06	77.18
MINIMUM UNIFORMITY (%)	95.66	85.4	85.53	84.02	83.55	82.85	80.8	77.81	72.22
CONTRAST (%)	2.92	6.16	13.66	15.29	110.29	7.85	6.67	7.41	37.83
CNR	1.95	0.93	0.42	0.37	0.05	0.73	0.85	0.77	0.15
MAXIMUM HU DEVIATION (HU)	257.43	349.29	450.86	437.65	487.49	509.45	609.24	612.65	659.22

**Table 3.1 :Intrafraction small field size 5mm to 45 mm**

Intrafraction Field Size SMALL (mm)										
PARAMETER	REF VALUE	5 mm	10mm	15mm	20mm	25mm	30mm	35mm	40mm	45mm
GEOMETRIC DISTORTION (mm)	-0.42	-0.72	-0.49	-0.39	-0.5	-0.6	-0.65	-0.7	-0.8	-0.83
SPATIAL RESOLUTION (lp/mm)	0.27	0.41	0.37	0.3	0.3	0.31	0.35	0.33	0.29	0.28
OVERALL UNIFORMITY (%)	95.76	96.76	96.43	96.97	96.14	95.34	95.13	95.19	94.12	93.17
MINIMUM UNIFORMITY (%)	95.66	96.69	96.34	96.91	96.04	95.19	94.96	95.01	93.87	92.79
CONTRAST (%)	2.92	5.49	4.77	4.67	6.0	5.08	6.09	15.74	9.36	4.21
CNR	1.95	1.04	1.19	1.22	0.95	1.12	0.094	0.36	0.61	1.35
MAXIMUM HU DEVIATION (HU)	257.43	255.35	251.67	258.31	269.55	261.98	263.16	271.08	287	312.86

**Table 3.2: Intrafraction small field size from 50 to 90 mm**

Intrafraction Field Size SMALL (mm)									
PARAMETER	REF VALUE	50mm	55mm	60mm	65mm	70mm	75mm	80mm	90mm
GEOMETRIC DISTORTION (mm)	-0.42	-0.86	-0.91	-0.97	-1.18	-1.25	-1.45	-2.5	-7.99
SPATIAL RESOLUTION (lp/mm)	0.27	0.32	0.31	0.29	0.3	0.32	0.31	0.3	0.28
OVERALL UNIFORMITY (%)	95.76	92.39	90.51	89.38	89.56	89.47	88.01	86.86	84.03
MINIMUM UNIFORMITY (%)	95.66	91.39	89.8	88.43	88.7	88.55	86.81	85.35	81.78
CONTRAST (%)	2.92	47.82	50	10.62	14.11	11	12.81	15.41	9.01
CNR	1.95	0.12	0.12	0.54	0.4	0.52	0.45	0.37	0.63
MAXIMUM HU DEVIATION (HU)	257.43	313.49	302.82	349.39	330.37	376.02	403.55	447.18	452.84

**Fig 3.1 Geometric distortion (GD) for small and large intrafraction field size**

From figure 3.1 it is observed that Geometric distortion decreases as the intrafraction field size increases. It also improves diagnostic accuracy and help with therapeutic decision making. Spatial resolution is a critical factor in determining the level of detail in an image. It influences how clearly fine details can be captured and analyzed. Here we find from figure 3.2 Spatial resolution showing maximum 0.21lp/mm at large intrafraction field size 45mm. This indicates that larger fields can enhance the ability to resolve finer details, but this gain is offset by simultaneous losses in uniformity and CNR.

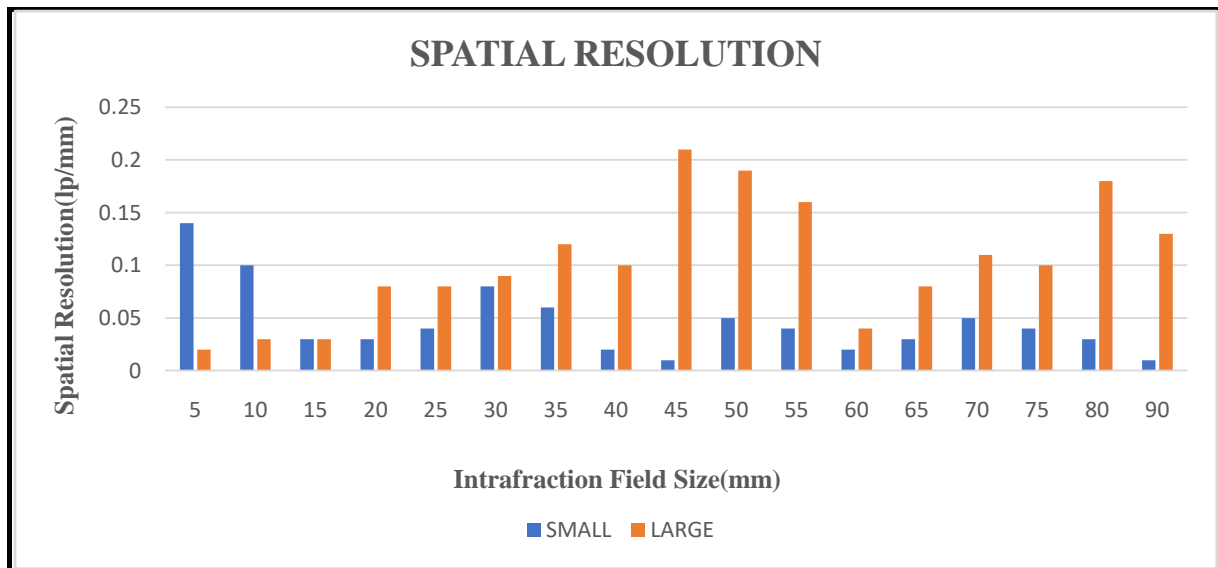


**Fig 3.2 Spatial Resolution (SR) for small and large intrafraction field size**

Overall uniformity in cone-beam computed tomography (CBCT) images can be quantified by measuring the consistency of pixel values across a region of interest (ROI). Overall uniformity in the context of imaging and digital systems refers to the consistency and evenness of the characteristics or features of an image or system. It implies that the image or the system behaves or appears consistently across the entire field or area without significant variation in quality, performance, or appearance.

From the table 2.1 it is found that overall Uniformity is approximately decreased with increasing field size. Overall and minimum uniformity decreased consistently with field size. Large-field scans showed the steepest decline, falling from ~96% at 5 mm to ~77% at 90 mm (Table 2.1).

Small fields maintained >90% uniformity up to 50 mm but degraded below 85% at 90 mm (Table 3.1). These results suggest that reduced intrafraction field size imaging should be prioritized to preserve uniformity, especially when soft tissue contrast is clinically important.

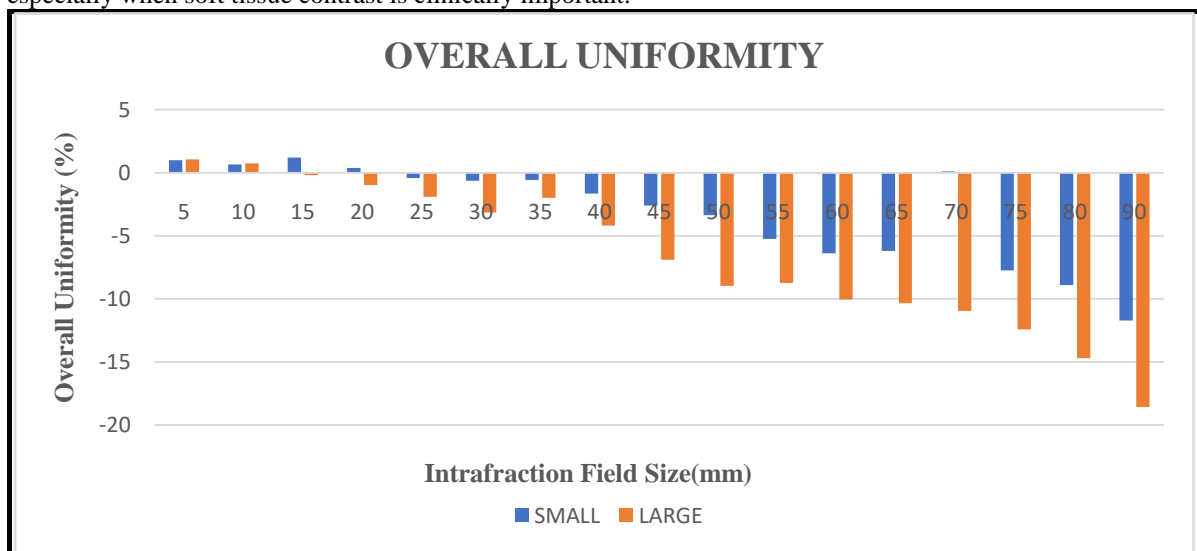


**Fig 3.3 Overall Uniformity for small and large intrafraction field size**

Contrast in an image refers to the difference between the lightest and darkest areas. High contrast images have a wide range between light and dark, making the details stand out more, while low contrast images have a more gradual transition between light and dark areas, creating a softer or more muted look.

Also from the table 2.1 it is seen that contrast approximately increases as intrafraction field size increases.

Contrast-to-noise ratio (CNR) is a quantitative measure of image quality in cone beam computed tomography (CBCT) that can affect the accuracy of diagnostic information. CNR is the ratio of the difference in signal (contrast) to the amount of noise in an image.

CNR is an important tool for determining image quality and is often used in place of signal-to-noise ratio (SNR) in CT and MRI imaging. It is a measure of image quality established on a contrast.



It is desirable for an imaging technology to obtain images with advanced image quality, indicating sufficient contrast-to-noise ratio (CNR) efficiency and soft-tissue differentiation, while impairing the necessary radiation dose.

From the table 2.1 it is observed that CNR is approximately decreased with increasing intrafraction field size. Hounsfield unit (HU) values in cone-beam computed tomography (CBCT) images can be inaccurate and affect the accuracy of dose calculations for radiotherapy. The figure 3.4 shows that Maximum HU deviation increases with increasing field size.

**Fig 3.4 Maximum HU Deviation for large and small intrafraction field size**

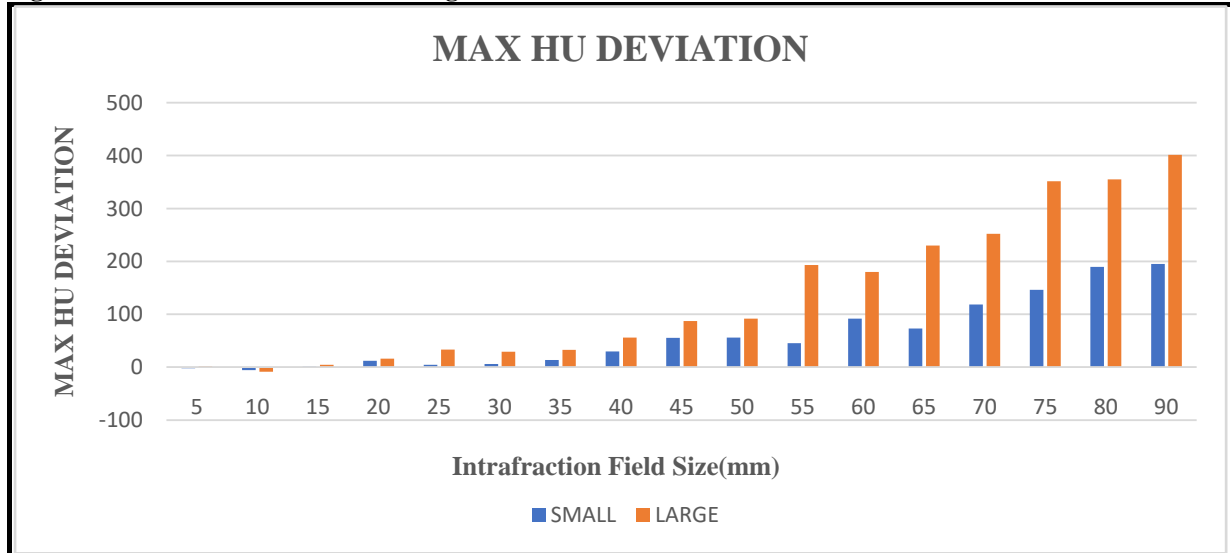


**Fig 3.4 Maximum HU Deviation for small and large intrafraction field size**

#### Comparison Between Small and Large Fields

Small-field intrafraction CBCT demonstrated superior image stability, with lower geometric distortion, better uniformity, and smaller HU deviations than large-field acquisitions. While large fields offered slightly better spatial resolution, their rapid loss of uniformity and accuracy limited their practical clinical value.

#### Suggested Improvements

The results underscore the need for scatter reduction techniques, such as optimized field size selection, use of anti-scatter grids, or advanced reconstruction algorithms, to improve image stability. Prior reports have shown that applying iterative and limited-angle reconstructions can mitigate distortion and noise during treatment imaging.

#### Clinical Implications

Overall, this study demonstrates that intrafraction CBCT imaging is clinically feasible for SBRT, particularly for small and mid-range field sizes. Larger fields compromise accuracy due to distortion, uniformity loss, and HU errors, despite modest gains in resolution and contrast. Careful optimization of acquisition protocols can enhance the reliability of intrafraction CBCT, enabling improved motion monitoring, adaptive response, and ultimately more precise radiation delivery.

#### DISCUSSION

The aim of this research paper was to understand the effect of MV scatter on real time intrafraction CBCT imaging and provide imaging recommendation based on treatment field size and imaging parameter.

This was done by investigating the image quality from intrafraction CBCT acquisitions for different field size and it was compared against reference CBCT scans (without MV beam ON) with the help of My QA Software. Graphs are plotted with normalized data.

The finding of this study was that intrafraction CBCT image quality decreased as MV field size increased because mv scatter increase as field size increases. Various parameters like Geometric distortion (GD), Spatial resolution, Minimum Uniformity, Overall Uniformity, Contrast, CNR and Maximum HU Deviations shown different effect. Geometric distortion progressively decreased with small and large intrafraction field size reaching values as high as -1.95 mm in large field (90mm large) and -7.99 mm in small field acquisitions. Increasing geometric distortion means less accuracy, which can lead to missed diagnosis, incorrect measurements and treatment errors. A decrease geometric distortion means more accuracy, it leads to better outcomes in diagnosis, treatment planning and image guided intervention upto 80 mm field size can be clinically used.

In table 2.1 (large field size 5 mm to 45 mm) and table 2.2 (large field size 50 mm to 90 mm) the geometric distortion reduces from -0.66 mm to -1.95 mm, indicating improved imaging accuracy with larger field sizes from which better outcomes achieved.

Spatial resolution was approximately increased for both small and large intrafraction field size indicating that the system can resolve finer details when scanning larger volumes. It influences clinical

decision making, suggesting that choosing a larger field size could be beneficial when high detail imaging is required.

High spatial resolution enhances the detection of small lesions (e.g., micro calcifications in breast cancer or early lung nodules), improves visualization of fine fractures, and offers clearer images in modalities like CT, MRI, and ultrasound, aiding in the accurate assessment of tumor margins, vascular anomalies, and small anatomical structures. Conversely, decreased spatial resolution leads to blurred images where small details may be lost, increasing the risk of missed lesions or tumors, poorly defined tumor borders, and inaccurate treatment planning, particularly in critical surgeries or multi-modality imaging like PET/CT and MRI/CT fusion, where precise anatomical overlay is essential for effective diagnosis, monitoring, and intervention.

Overall Uniformity approximately decreases with increasing intrafraction field sizes. This is due to increased MV scatter and beam hardening which can degrade image quality and affect clinical diagnosis. From the fig 3.3 upto 40 mm intrafraction field size, overall uniformity is <-5%.

While higher resolution enhances fine detail visualization, this benefit was undermined by concurrent declines in overall uniformity, CNR, and HU accuracy, which are essential for accurate target localization and tissue differentiation.

Image contrast exhibited variable behavior across field sizes, with several peaks likely influenced by anatomical heterogeneities within the phantom and differences in beam modulation. However, CNR—a more robust indicator of image quality—declined steadily as field size increased. This suggests that while localized contrast may improve in some conditions, the accompanying increase in noise diminishes diagnostic clarity and may impair target tracking, especially in soft-tissue-dominated regions like the abdomen or pelvis.

From the figure 3.4(normalized graph) it is seen that Maximum HU deviation increased significantly with intrafraction field size, upto 50 mm intrafraction large and small field size max HU deviation is <100. For 90 mm intrafraction large field size Maximum HU deviation is 400 while for small intrafraction field size Maximum HU deviation is 200. Since HU values are critical for electron density estimation and adaptive planning, such deviations render real-time CBCT less reliable for dose recalculation or plan adaptation under large-field conditions. For SBRT and stereotactic radiosurgery (SRS), where tight dose gradients are involved, maintaining HU integrity is vital. Therefore, the use of real-time intrafraction CBCT in adaptive workflows should be restricted to field sizes that ensure HU deviations remain within clinically acceptable limits (<100 HU recommended for dosimetric accuracy).

### Clinical Feasibility and Future Implementation

This commissioning study validates the feasibility of real-time intrafraction CBCT in the clinical setting, particularly for SBRT applications requiring high spatial accuracy and real-time motion management. The integration of this technology allows for intra-beam imaging, enabling visualization of target displacement during actual radiation delivery—a major advancement over pre-treatment CBCT or retrospective monitoring.

However, implementation should be selective. Imaging protocols must be optimized to account for MV scatter—possibly through anti-scatter grids, improved kV/MV timing synchronization, or software-based scatter correction algorithms. Furthermore, iterative reconstruction techniques and AI-enhanced post-processing may help recover image quality even under high-scatter conditions.

### Study Limitations and Directions for Future Research

The clinical feasibility assessment did not incorporate real patient data or clinical outcomes, which are essential for a comprehensive and realistic evaluation. To strengthen future research, subsequent validation studies should include real-world patient data and outcome measures. This will enable a more accurate assessment of the intervention's effectiveness, safety, and practical applicability in actual clinical settings.

### CONCLUSION

This study shows that real-time intrafraction CBCT is a practical and promising tool for improving accuracy during SBRT treatments. However, as the radiation field size increases, image quality tends to get worse—leading to more distortion, reduced contrast, and less reliable CT numbers. These effects are caused by increased MV scatter during treatment, which interferes with CBCT image quality. Our results suggest that using small to mid-sized fields can provide a better balance between treatment coverage and image clarity, helping clinicians track tumor motion more accurately in real time. This is especially important for adaptive radiotherapy, where treatment is adjusted based on daily imaging. Real-time intrafraction CBCT imaging, with careful optimization of field size and imaging parameters, can enhance treatment precision and patient outcomes in radiotherapy.

### REFERENCES

1. Jaffray DA, Das S, Jacobs PM, Jeraj R, Lambin P. How advances in imaging will affect precision radiation oncology. *International Journal of Radiation Oncology\* Biology\* Physics*. 2018 Jun 1;101(2):292-8.
2. Cyran CC, Paprottka PM, Eisenblätter M, Clevert DA, Rist C, Nikolaou K, Lauber K, Wenz F, Hausmann D, Reiser MF, Belka C. Visualization, imaging and new preclinical diagnostics in radiation oncology. *Radiation Oncology*. 2014 Dec;9:1-5.

3. Dawson LA, Ménard C. Imaging in radiation oncology: a perspective. *The oncologist*. 2010 Apr 1;15(4):338-49.
4. Sterzing F, Engenhart-Cabillic R, Flentje M, Debus J. Image-guided radiotherapy: a new dimension in radiation oncology. *DeutschesAerzteblatt International*. 2011 Apr 22;108(16):274.
5. West CM, Huddart RA. Biomarkers and imaging for precision radiotherapy. *Clinical Oncology*. 2015 Oct 1;27(10):545-6.
6. Tree AC, Khoo VS, Eeles RA, Ahmed M, Dearnaley DP, Hawkins MA, Huddart RA, Nutting CM, Ostler PJ, van As NJ. Stereotactic body radiotherapy for oligometastases. *The lancet oncology*. 2013 Jan 1;14(1):e28-37.
7. Corbin KS, Hellman S, Weichselbaum RR. Extracranial oligometastases: a subset of metastases curable with stereotactic radiotherapy. *Journal of Clinical Oncology*. 2013 Apr 10;31(11):1384-90.
8. Chang JY, Senan S, Paul MA, Mehran RJ, Louie AV, Balter P, Groen HJ, McRae SE, Widder J, Feng L, van den Borne BE. Stereotactic ablative radiotherapy versus lobectomy for operable stage I non-small-cell lung cancer: a pooled analysis of two randomised trials. *The lancet oncology*. 2015 Jun 1;16(6):630-7.
9. Jaffray DA. Image-guided radiotherapy: from current concept to future perspectives. *Nature reviews Clinical oncology*. 2012 Dec;9(12):688-99.
10. Beltran C, Herman MG, Davis BJ. Planning target margin calculations for prostate radiotherapy based on intrafraction and interfraction motion using four localization methods. *International Journal of Radiation Oncology\* Biology\* Physics*. 2008 Jan 1;70(1):289-95.
11. Litzenberg DW, Balter JM, Hadley SW, Sandler HM, Willoughby TR, Kupelian PA, Levine L. Influence of intrafraction motion on margins for prostate radiotherapy. *International Journal of Radiation Oncology\* Biology\* Physics*. 2006 Jun 1;65(2):548-53.
12. Keall PJ, Lauve AD, Hagan MP, Siebers JV. A strategy to correct for intrafraction target translation in conformal prostate radiotherapy: Simulation results. *Medical physics*. 2007 Jun;34(6Part1):1944-51.
13. Li HS, Chetty IJ, Enke CA, Foster RD, Willoughby TR, Kupellian PA, Solberg TD. Dosimetric consequences of intrafraction prostate motion. *International Journal of Radiation Oncology\* Biology\* Physics*. 2008 Jul 1;71(3):801-12.
14. Krupa A, Fichtinger G, Hager GD. Real-time tissue tracking with B-mode ultrasound using speckle and visual servoing. In *Medical Image Computing and Computer-Assisted Intervention—MICCAI 2007: 10th International Conference, Brisbane, Australia, October 29–November 2, 2007, Proceedings, Part II* 10 2007 (pp. 1-8). Springer Berlin Heidelberg.
15. Kotte AN, Hofman P, Lagendijk JJ, van Vulpen M, van der Heide UA. Intrafraction motion of the prostate during external-beam radiation therapy: analysis of 427 patients with implanted fiducial markers. *International Journal of Radiation Oncology\* Biology\* Physics*. 2007 Oct 1;69(2):419-25.
16. Madsen BL, Hsi RA, Pham HT, Presser J, Esagui L, Corman J, Myers L, Jones D. Intrafractional stability of the prostate using a stereotactic radiotherapy technique. *International Journal of Radiation Oncology\* Biology\* Physics*. 2003 Dec 1;57(5):1285-91.
17. Langen KM, Willoughby TR, Meeks SL, Santhanam A, Cunningham A, Levine L, Kupelian PA. Observations on real-time prostate gland motion using electromagnetic tracking. *International Journal of Radiation Oncology\* Biology\* Physics*. 2008 Jul 15;71(4):1084-90.
18. Lagendijk JJ, Raaymakers BW, Raaijmakers AJ, Overweg J, Brown KJ, Kerkhof EM, van der Put RW, Hårdemark B, van Vulpen M, van der Heide UA. MRI/linac integration. *Radiotherapy and Oncology*. 2008 Jan 1;86(1):25-9.
19. Boda-Heggemann J, Köhler FM, Wertz H, Ehmann M, Hermann B, Riesenacker N, Küpper B, Lohr F, Wenz F. Intrafraction motion of the prostate during an IMRT session: a fiducial-based 3D measurement with Cone-beam CT. *Radiation oncology*. 2008 Dec;3:1-8.
20. Western C, Hristov D, Schlosser J. Ultrasound imaging in radiation therapy: from interfractional to intrafractional guidance. *Cureus*. 2015 Jun 20;7(6).
21. O'Shea T, Bamber J, Fontanarosa D, Van Der Meer S, Verhaegen F, Harris E. Review of ultrasound image guidance in external beam radiotherapy part II: intra-fraction motion management and novel applications. *Physics in medicine & biology*. 2016 Mar 22;61(8):R90.
22. Spadea MF, Tagaste B, Riboldi M, Preve E, Alterio D, Piperno G, Garibaldi C, Orecchia R, Pedotti A, Baroni G. Intra-fraction setup variability: IR optical localization vs. X-ray imaging in a hypofractionated patient population. *Radiation oncology*. 2011 Dec;6:1-8.
23. Mail TB. Catphan® 500 and 600 Product Guide.
24. Seltzer S. XCOM-photon cross sections database, NIST standard reference database 8. (No Title). 1987 Jan 1.
25. O'Shea T, Bamber J, Fontanarosa D, Van Der Meer S, Verhaegen F, Harris E. Review of ultrasound image guidance in external beam radiotherapy part II: intra-fraction motion management and novel applications. *Physics in medicine & biology*. 2016 Mar 22;61(8):R90.